

Optimal Least-Squares Estimator and Precoder for Energy Beamforming over IQ-Impaired Channels

Deepak Mishra, *Member, IEEE*, and Håkan Johansson, *Senior Member, IEEE*

Abstract—Usage of low-cost hardware in large antenna arrays and low-power wireless devices in Internet-of-Things (IoT) has led to the degradation of practical beamforming gains due to the underlying hardware impairments like in-phase-and-quadrature-phase imbalance (IQI). To address this timely concern, we present a new nontrivial closed-form expression for the globally-optimal least-squares estimator (LSE) for the IQI-influenced channel between a multiantenna transmitter and single-antenna IoT device. Thereafter, to maximize the realistic transmit beamforming gains, a novel precoder design is derived that accounts for the underlying IQI for maximizing received power in both single and multiuser settings. Lastly, the simulation results, demonstrating a significant -8dB improvement in the mean-squared error of the proposed LSE over existing benchmarks, show that the optimal precoder designing is more critical than accurately estimating IQI-impaired channels. Also, the proposed jointly-optimal LSE and beamformer outperforms the existing designs by providing 24% enhancement in the mean signal power received under IQI.

Index Terms—Antenna array, IQ imbalance, channel estimation, hardware impairments, precoder, global optimization.

I. INTRODUCTION

Massive antenna array technology can help in realizing large beamforming and multiplexing gains [1], as desired for the goal of sustainable ubiquitous Internet-of-Things (IoT) deployment [2]. However, due to the usage of low-cost hardware components, the performance of these sustainable IoT systems is more prone to suffer from the radio frequency (RF) imperfections [3] like the in-phase-and-quadrature-phase-imbalance (IQI) [4]. Thus, generalized green signal processing techniques are being investigated to combat the adverse effect of hardware impairments [5]–[7] and the problem of carrier frequency offset (CFO) recovery in frequency-selective IQI [8]. However, as these impairments adversely influence both channel estimation (CE) and precoding processes at transmitter (TX), new jointly-optimal estimator and beamformer designs are required.

A. State-of-the-Art

In recent times, there have been increasing interests [4], [9]–[14] on investigating the performance degradation in energy beamforming (EB) gains of the massive multiple-input-single-output (MISO) systems suffering from IQI. Specifically, as each single-antenna receiver (RX) in multiuser (MU) systems gets wrongly viewed as having a virtual port due to underlying IQI [9], it leads to an inaccurate CE at the multiantenna TX.

D. Mishra and H. Johansson are with the Communication Systems Division of the Department of Electrical Engineering at the Linköping University, 581 83 Linköping, Sweden (emails: {deepak.mishra, hakan.johansson}@liu.se).

This research work is funded by ELLIIT.

Noting it, sum rate limits in downlink (DL) MU MISO systems under IQI and CE errors were derived in [10]. In contrast [11], [12] were targeted towards the joint CE and IQI compensation in uplink (UL) MISO systems. More recently, performance analysis of dual-hop statistical channel state information (CSI) assisted cooperative communications was conducted via simulations in [13] to incorporate the effect of IQI. However, these works [9]–[13] only presented linear-minimum-mean-square-error (LMMSE) [14] based CE, that requires strong prior CSI.

On another front, there are also some works on least-squares (LS) based CE under IQI [15]–[17]. A special structured pilot was used in [15] to obtain LS estimator (LSE) for both actual and IQI-based virtual signal terms. However, these complex pilots are not suited for limited feedback settings involving low-power IoT RX. Therefore, LS and LMMSE estimates using conventional methods were presented in [16] to quantify EB gains during MISO wireless power transfer under joint-TX-RX IQI and CE errors over Rician fading. Lately, an LSE using additional pilots to exploit the interference among symmetric subcarriers for mitigating effect of IQI was designed in [17].

B. Motivation and Scope

All existing works [9]–[17], investigating the impact of IQI on CE, considered the underlying additional virtual signal term as interference, and *simply ignored* the information content in it. Likewise, the current precoder designs for multiantenna TX serving single-antenna RX are based on *suboptimal* maximum ratio transmission (MRT) scheme, ignoring the impairment that signal undergoes due to IQI. *To the best of our knowledge, the optimal CE and TX precoder designs respectively minimizing the underlying LS error and maximizing signal power at RX under IQI and CE errors have not been investigated yet.*

Unlike existing works, the proposed *globally-optimal* LSE does not require any prior CSI. The adopted *novel and generic* complex-to-real-domain transformation based methodology to obtain the LSE and precoder in *closed-form* can be extended for investigating designs in MU and multiantenna RX settings. Lastly, the proposed precoder design holds for *any CE scheme*.

C. Contribution of This Letter

Our contribution is three-fold. (1) *Global-minimizer of LS error* during CE under TX-RX-IQI is derived in closed-form. (2) *Novel precoder design* is proposed to globally-maximize the nonconvex received signal power over IQI-impaired MISO channels. Extension of this design to multiuser settings is also discussed. (3) To validate the nontrivial analysis for different system parameters, extensive simulations are conducted, which

also *quantify the achievable EB gains* over benchmarks. After outlining system model in Section II, these three contributions are discussed in Sections III, IV, and V, respectively.

II. SYSTEM DESCRIPTION

In this section we present the system model details, followed by the adopted transmission protocol and IQI signal model.

A. Wireless Channel Model and Transmission Protocol

We consider DL MISO system comprising of an N antenna source \mathcal{S} and a single-antenna IoT user \mathcal{U} . Assuming flat quasi-static Rayleigh block fading [18, Ch 2.2], the \mathcal{U} -to- \mathcal{S} channel is represented by $\mathbf{h} \sim \mathcal{CN}(\mathbf{0}_{N \times 1}, \beta \mathbf{I}_N)$, where β incorporates the effect of both distance-dependent path loss and shadowing. Transmission protocol involves estimation of \mathbf{h} from the received IQI-impaired signal at \mathcal{S} . Exploiting channel reciprocity in the adopted time-division duplex mode [19], we can divide each coherence block of τ seconds (s) into two phases, namely CE and information transfer (IT). During CE phase of duration $\tau_c \leq \tau$, \mathcal{U} transmits a pilot signal s with mean power p_c and the resulting received baseband signal at \mathcal{S} without any IQI is

$$\mathbf{y} = \mathbf{h} s + \mathbf{n}, \quad (1)$$

where $\mathbf{n} \in \mathbb{C}^{N \times 1}$ is received additive white Gaussian noise (AWGN) vector with zero mean entries having variance σ_1^2 .

B. Adopted Transmission Protocol

Our protocol involves estimation of \mathbf{h} from the received IQI-impaired signal at \mathcal{S} . Here, exploiting channel reciprocity in the adopted time-division duplex mode [19], we can divide each coherence block into two phases, namely CE and information transfer (IT). During CE phase of duration $\tau_c \leq \tau$, \mathcal{U} transmits a pilot signal s with mean power p_c and the resulting received baseband signal $\mathbf{y} \in \mathbb{C}^{N \times 1}$ at \mathcal{S} without any IQI is

$$\mathbf{y} = \mathbf{h} s + \mathbf{n}, \quad (2)$$

where $\mathbf{n} \in \mathbb{C}^{N \times 1}$ is received additive white Gaussian noise (AWGN) vector with zero mean entries having variance σ_1^2 .

C. Signal Model for Characterizing IQ Impairments

We assume that received baseband signal \mathbf{y} in (2) undergoes the joint-TX-RX-IQI. Therefore, the baseband signal s at \mathcal{U} gets practically altered to s_T , defined below, due to TX-IQI [3]

$$s_T = T_{\mathcal{U}1} s + T_{\mathcal{U}2} s^*. \quad (3)$$

Here, $T_{\mathcal{U}1} \triangleq \frac{1+g_{T\mathcal{U}} e^{j\phi_{T\mathcal{U}}}}{2}$ and $T_{\mathcal{U}2} \triangleq \frac{1-g_{T\mathcal{U}} e^{j\phi_{T\mathcal{U}}}}{2}$, with $g_{T\mathcal{U}}$ and $\phi_{T\mathcal{U}}$ respectively denoting TX amplitude and phase mismatch at IoT user \mathcal{U} . Similarly, the baseband signal \mathbf{y} received at \mathcal{S} gets practically impaired due to RX-IQI as [3]

$$\mathbf{y}_R = \mathbf{R}_{S1} \mathbf{y} + \mathbf{R}_{S2} \mathbf{y}^*, \quad (4)$$

where i th diagonal entry of diagonal matrices \mathbf{R}_{S1} and \mathbf{R}_{S2} are $[\mathbf{R}_{S1}]_i \triangleq \frac{1+g_{R_{S_i}} e^{-j\phi_{R_{S_i}}}}{2}$ and $[\mathbf{R}_{S2}]_i \triangleq \frac{1-g_{R_{S_i}} e^{j\phi_{R_{S_i}}}}{2}$. Here $g_{R_{S_i}}$ and $\phi_{R_{S_i}}$ respectively denote the RX amplitude and phase mismatch at the i th antenna of \mathcal{S} . Finally, combining

(3) and (4) in (2), the baseband signal $\mathbf{y}_J \in \mathbb{C}^{N \times 1}$ as received at \mathcal{S} during CE phase under joint-TX-RX-IQI is given by

$$\mathbf{y}_J = \mathbf{h}_A s + \mathbf{h}_B s^* + \mathbf{n}_J, \quad (5)$$

where $\mathbf{h}_A \triangleq \mathbf{R}_{S1} \mathbf{h} T_{\mathcal{U}1} + \mathbf{R}_{S2} \mathbf{h}^* T_{\mathcal{U}2}^*$, $\mathbf{h}_B \triangleq \mathbf{R}_{S1} \mathbf{h} T_{\mathcal{U}2} + \mathbf{R}_{S2} \mathbf{h}^* T_{\mathcal{U}1}^*$, and $\mathbf{n}_J \triangleq \mathbf{R}_{S1} \mathbf{n} + \mathbf{R}_{S2} \mathbf{n}^*$. We recall that for addressing the demands of low-rate IoT settings using narrow band signals [10], [12], we have adopted this frequency-independent-IQI model [3]. Furthermore, as the IQI parameters change very slowly as compared to the channel estimates, we assume their perfect knowledge availability at \mathcal{S} [3], [4], [9]–[12]. Using this practically-motivated assumption, we optimally exploit the information available in the IQI-based virtual signal term $\mathbf{h}_B s^*$ for designing the LSE and precoder at \mathcal{S} . Moreover, using this IQI-knowledge, our proposed solution methodology can also be applied to the frequency-dependent-IQI scenarios.

III. OPTIMAL CHANNEL ESTIMATION

A. Existing LSE $\hat{\mathbf{h}}_A$ for IQI-Impaired Channels

Current works [9]–[17] considered $\mathbf{h}_B s^* + \mathbf{n}_J$ as the effective noise signal under IQI, and thus, applied conventional pseudo-inverse method [20] on \mathbf{y}_J in (5) with $\|s\|^2 = p_c \tau_c$, to obtain LSE $\hat{\mathbf{h}}_A$ for the effective channel \mathbf{h}_A under IQI, defined below

$$\hat{\mathbf{h}}_A = \mathbf{y}_J s^* (s s^*)^{-1} = \mathbf{h}_A + \tilde{\mathbf{h}}_A, \quad (6)$$

where $\tilde{\mathbf{h}}_A \triangleq (\mathbf{h}_B s^* + \mathbf{n}_J) s^* (p_c \tau_c)^{-1}$ is underlying CE error.

B. Proposed LS Approach and Challenges

As mentioned in Section I-B, we consider both the terms in \mathbf{y}_J , i.e., actual $\mathbf{h}_A s$ and IQI-based virtual $\mathbf{h}_B s^*$, containing information on \mathbf{h} . Therefore, the proposed optimal LSE $\hat{\mathbf{h}}$ for \mathbf{h} can be obtained by solving the following LS problem in \mathbf{h} ,

$$\mathcal{O}_1 : \underset{\mathbf{h}}{\text{argmin}} \quad \mathcal{E} \triangleq \|\mathbf{y}_J - \mathbf{h}_A s - \mathbf{h}_B s^*\|^2.$$

Although \mathcal{O}_1 is nonconvex due to the presence of \mathbf{h}^* terms in \mathbf{h}_A and \mathbf{h}_B , we can characterize all the possible candidates for the optimal solution of \mathcal{O}_1 by setting derivative of objective \mathcal{E} to zero and then solve in \mathbf{h} . Below, we first simplify \mathcal{E} as

$$\mathcal{E} = \mathbf{y}_J^H \mathbf{y}_J - \mathbf{y}_J^H \mathbf{A} \mathbf{h} - \mathbf{y}_J^H \mathbf{B} \mathbf{h}^* + \mathbf{h}^H \mathbf{A}^H \mathbf{A} \mathbf{h} - \mathbf{h}^H \mathbf{A}^H \mathbf{y}_J + \mathbf{h}^H \mathbf{A}^H \mathbf{B} \mathbf{h}^* - \mathbf{h}^T \mathbf{B}^H \mathbf{y}_J + \mathbf{h}^T \mathbf{B}^H \mathbf{A} \mathbf{h} + \mathbf{h}^T \mathbf{B}^H \mathbf{B} \mathbf{h}^*, \quad (7)$$

where $\mathbf{A} \triangleq \mathbf{R}_{S1} T_{\mathcal{U}1} s + \mathbf{R}_{S1} T_{\mathcal{U}2} s^*$ and $\mathbf{B} \triangleq \mathbf{R}_{S2} T_{\mathcal{U}2} s + \mathbf{R}_{S2} T_{\mathcal{U}1} s^*$ are diagonal matrices. Using complex-valued differentiation rules [21] to the find derivative of (7) with respect to \mathbf{h} and setting resultant to zero, gives the following system

$$\mathbf{h}^H \mathbf{Z}_A + \mathbf{h}^T \mathbf{Z}_B = \mathbf{y}_{AB}^T, \quad (8)$$

where $\mathbf{y}_{AB} \triangleq \mathbf{A}^T \mathbf{y}_J^* + \mathbf{B}^H \mathbf{y}_J \in \mathbb{C}^{N \times 1}$ and $\mathbf{Z}_B \triangleq \mathbf{B}^H \mathbf{A} + \mathbf{A}^T \mathbf{B}^* \in \mathbb{C}^{N \times N}$. Here, $\mathbf{Z}_A \triangleq \mathbf{A}^H \mathbf{A} + \mathbf{B}^T \mathbf{B}^* \in \mathbb{R}^{N \times N}$ is a diagonal matrix with $[\mathbf{Z}_A]_i = |[\mathbf{A}]_i|^2 + |[\mathbf{B}]_i|^2$, $\forall i \in \mathcal{N} = \{1, 2, \dots, N\}$.

Though, we have been able to reduce the LS problem \mathcal{O}_1 of obtaining optimal LSE $\hat{\mathbf{h}}$ for IQI-impaired channels to the nonlinear system of equations (8) in the complex variable \mathbf{h} , solving the latter numerically is computationally-expensive and time-consuming, especially for $N \gg 1$. Therefore, next we propose an *equivalent* complex-to real transformation for *efficiently* obtaining unique globally-optimal solution $\hat{\mathbf{h}}$ of \mathcal{O}_1 .

C. Closed-Form Expression for Globally-Optimal LSE $\hat{\mathbf{h}}$

Before deriving $\hat{\mathbf{h}}$, let us define some key notations below.

Definition 1: We can define the real composite representations for any complex vector $\mathbf{u} \in \mathbb{C}^{n \times 1}$ by $\underline{\mathbf{u}} \in \mathbb{R}^{2n \times 1}$ and for any complex matrix $\mathbf{U} \in \mathbb{C}^{n_1 \times n_2}$ by $\underline{\mathbf{U}} \in \mathbb{R}^{2n_1 \times 2n_2}$ as below

$$\underline{\mathbf{u}} \triangleq \begin{bmatrix} \text{Re}\{\mathbf{u}\} \\ \text{Im}\{\mathbf{u}\} \end{bmatrix}, \quad \underline{\mathbf{U}} \triangleq \begin{bmatrix} \text{Re}\{\mathbf{U}\} & -\text{Im}\{\mathbf{U}\} \\ \text{Im}\{\mathbf{U}\} & \text{Re}\{\mathbf{U}\} \end{bmatrix}. \quad (9)$$

Using above definition, (8) can be rewritten in real-domain as

$$\begin{bmatrix} \mathbf{Z}_A & \mathbf{0}_{N \times N} \\ \mathbf{0}_{N \times N} & -\mathbf{Z}_A \end{bmatrix} \underline{\mathbf{h}} + \underline{\mathbf{Z}}_B \underline{\mathbf{h}} = \underline{\mathbf{y}}_{AB}. \quad (10)$$

Recalling \mathbf{Z}_A is real while solving (10), the real and imaginary terms of the proposed LSE $\hat{\mathbf{h}}$ can be analytically expressed as

$$\begin{bmatrix} \text{Re}\{\hat{\mathbf{h}}\} \\ \text{Im}\{\hat{\mathbf{h}}\} \end{bmatrix} \triangleq \begin{bmatrix} \mathbf{Z}_A + \text{Re}\{\mathbf{Z}_B\} & -\text{Im}\{\mathbf{Z}_B\} \\ \text{Im}\{\mathbf{Z}_B\} & -\mathbf{Z}_A + \text{Re}\{\mathbf{Z}_B\} \end{bmatrix}^{-1} \underline{\mathbf{y}}_{AB}. \quad (11)$$

IV. OPTIMAL TRANSMIT BEAMFORMING DESIGN

After optimizing LSE using CE phase, now we optimize the efficiency of IT (phase 2) over IQI-impaired DL channel. Metric to be maximized here by optimally designing precoder $\mathbf{x} \in \mathbb{C}^{N \times 1}$ at \mathcal{S} is the *signal power at \mathcal{U}* during IT phase.

A. Conventional Precoder Design

With s_U being unit-energy data symbol, the signal received at \mathcal{U} due to IT, under perfect CSI and no IQI assumption, is

$$y_U = \mathbf{h}^T \mathbf{x} s_U + n_U, \quad (12)$$

where precoder \mathbf{x} satisfies $\|\mathbf{x}\|^2 \leq p_i$, with p_i being the transmit power of \mathcal{S} and $n_U \sim \mathcal{CN}(0, \sigma_2^2)$ is the received AWGN at \mathcal{U} . Like in case of CE, the existing works [9]–[17] ignored the virtual term and designed the precoder as in conventional systems to perform MRT at \mathcal{S} in the DL. Therefore, using the conventional LSE $\hat{\mathbf{h}}_A$ as defined in Section III-A, the benchmark precoder following MRT is given by $\mathbf{x}_A \triangleq \frac{\sqrt{p_i} \hat{\mathbf{h}}_A^*}{\|\hat{\mathbf{h}}_A\|}$.

B. Maximizing Received Signal Strength under IQI

Under joint-TX-RX-IQI, y_U gets practically impaired to

$$y_{UJ} = R_{U1} y_{UT} + R_{S2} y_{UT}^* = \mathbf{a} \mathbf{x} + \mathbf{b} \mathbf{x}^* + n_{UJ}, \quad (13)$$

where complex vectors \mathbf{a} , \mathbf{b} , and n_{UJ} are defined below

$$\mathbf{a} \triangleq (R_{U1} \mathbf{h}^T \mathbf{T}_{S1} + R_{U2} \mathbf{h}^H \mathbf{T}_{S2}^*) s_U \in \mathbb{C}^{1 \times N}, \quad (14a)$$

$$\mathbf{b} \triangleq (R_{U1} \mathbf{h}^T \mathbf{T}_{S2} + R_{U2} \mathbf{h}^H \mathbf{T}_{S1}^*) s_U^* \in \mathbb{C}^{1 \times N}, \quad (14b)$$

$$n_{UJ} \triangleq R_{U1} n_U + R_{S2} n_U^* \sim \mathcal{CN}(0, \sigma_J^2). \quad (14c)$$

Here with g_{R_U} and ϕ_{R_U} respectively denoting RX amplitude and phase mismatch at \mathcal{U} , $R_{U1} \triangleq \frac{1+g_{R_U} e^{-j\phi_{R_U}}}{2}$ and $R_{U2} \triangleq \frac{1-g_{R_U} e^{j\phi_{R_U}}}{2}$. Therefore, $\sigma_J^2 \triangleq (|R_{U1}|^2 + |R_{U2}|^2) \sigma_2^2$. $y_{UT} \triangleq \mathbf{h}^T (\mathbf{T}_{S1} \mathbf{x} s_U + \mathbf{T}_{S2} \mathbf{x}^* s_U^*) + n_U$ is TX-IQI impaired signal, where \mathbf{T}_{S1} and \mathbf{T}_{S2} represent diagonal matrices with $g_{T_{S_i}}$ and $\phi_{T_{S_i}}$ in their i th diagonal entries $[\mathbf{T}_{S1}]_i \triangleq \frac{1+g_{T_{S_i}} e^{j\phi_{T_{S_i}}}}{2}$ and $[\mathbf{T}_{S2}]_i \triangleq \frac{1-g_{T_{S_i}} e^{j\phi_{T_{S_i}}}}{2}$ respectively denoting TX amplitude and phase mismatch at i th antenna of \mathcal{S} during the IT phase.

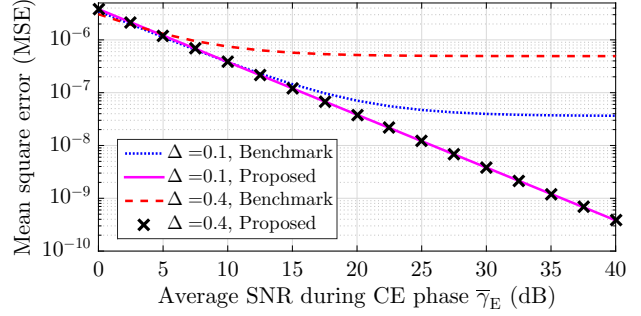


Fig. 1. Validating LSE $\hat{\mathbf{h}}$ against benchmark for different SNR and IQI values.

Noting that the received signal has two useful terms $\mathbf{a} \mathbf{x}$ and $\mathbf{b} \mathbf{x}^*$ in (13), the proposed precoder optimization problem for maximizing the signal power at \mathcal{U} is formulated as below

$$\mathcal{O}_2: \underset{\mathbf{x}}{\text{argmax}} \|\mathbf{a} \mathbf{x} + \mathbf{b} \mathbf{x}^*\|^2, \quad \text{subject to (C1)}: \|\mathbf{x}\|^2 \leq p_i.$$

The challenges here include non-convexity of \mathcal{O}_2 and need for fast-converging or closed-form globally-optimal design to obtain the desired solution \mathbf{x}_o in a computationally-efficient manner. Furthermore, this signal power as objective is actually closely-related to other *key metrics* like ergodic capacity and detection error probability [22] because former's higher value also implies better ergodic capacity or lower error probability.

C. Novel Globally-Optimal Precoder

Though \mathcal{O}_2 is nonconvex, its globally-optimal solution can be characterized via Karush-Kuhn-Tucker (KKT) point [23]. To obtain latter, below we define Lagrangian function for \mathcal{O}_2

$$\mathcal{L} \triangleq \|\mathbf{a} \mathbf{x} + \mathbf{b} \mathbf{x}^*\|^2 - \ell (\|\mathbf{x}\|^2 - p_i) = \mathbf{x}^H \mathbf{a}^H \mathbf{a} \mathbf{x} + \mathbf{x}^H \mathbf{a}^H \mathbf{b} \mathbf{x}^* + \mathbf{x}^T \mathbf{b}^H \mathbf{a} \mathbf{x} + \mathbf{x}^T \mathbf{b}^H \mathbf{b} \mathbf{x}^* - \ell (\mathbf{x}^H \mathbf{x} - p_i), \quad (15)$$

where $\ell \geq 0$ is the Lagrange multiplier corresponding to (C1).

$$\frac{\partial \mathcal{L}}{\partial \mathbf{x}} = \mathbf{x}^H \mathbf{a}^H \mathbf{a} + \mathbf{x}^T (\mathbf{b}^H \mathbf{a} + \mathbf{a}^T \mathbf{b}^*) + \mathbf{x}^T \mathbf{b}^H \mathbf{b} - \ell \mathbf{x}^H. \quad (16)$$

Setting $\frac{\partial \mathcal{L}}{\partial \mathbf{x}}$ in (16) to $\mathbf{0}_{1 \times N}$, yields the KKT condition below

$$\mathbf{x}^T \mathbf{Z}_a^* + \mathbf{x}^H \mathbf{Z}_b^* = \ell \mathbf{x}^T, \quad (17)$$

where $\mathbf{Z}_a \triangleq \mathbf{a}^H \mathbf{a} + \mathbf{b}^T \mathbf{b}^*$ and $\mathbf{Z}_b \triangleq \mathbf{b}^H \mathbf{a} + \mathbf{a}^T \mathbf{b}^*$. Using the composite real definition from Section III-C in (17), we obtain

$$(\underline{\mathbf{Z}}_a)^* \underline{\mathbf{x}} + (\underline{\mathbf{Z}}_b)^H \begin{bmatrix} \text{Re}\{\mathbf{x}\} \\ -\text{Im}\{\mathbf{x}\} \end{bmatrix} = \ell \underline{\mathbf{x}}, \quad \text{or } \underline{\mathbf{Z}}_{ab} \underline{\mathbf{x}} = \ell \underline{\mathbf{x}}, \quad (18)$$

where the real square matrix $\underline{\mathbf{Z}}_{ab} \in \mathbb{R}^{2N \times 2N}$ is defined as

$$\underline{\mathbf{Z}}_{ab} \triangleq \begin{bmatrix} \text{Re}\{\mathbf{Z}_a\} + \text{Re}\{\mathbf{Z}_b\} & \text{Im}\{\mathbf{Z}_a\} + \text{Im}\{\mathbf{Z}_b\} \\ -\text{Im}\{\mathbf{Z}_a\} + \text{Im}\{\mathbf{Z}_b\} & \text{Re}\{\mathbf{Z}_a\} - \text{Re}\{\mathbf{Z}_b\} \end{bmatrix}. \quad (19)$$

As (18) possesses an eigenvalue problem form, the solution to (18) in $\underline{\mathbf{x}}$ is given by the principal eigenvector $\mathbf{v}_{\max}\{\underline{\mathbf{Z}}_{ab}\}$ corresponding to the maximum eigenvalue $\lambda_{\max}\{\underline{\mathbf{Z}}_{ab}\}$ of $\underline{\mathbf{Z}}_{ab}$. Therefore, the globally-maximum signal power is attained at the proposed precoder $\mathbf{x}_o \triangleq \text{Re}\{\mathbf{x}_o\} + j \text{Im}\{\mathbf{x}_o\}$, whose real and imaginary parts, obtained via eigen-decomposition are

$$\underline{\mathbf{x}}_o = \begin{bmatrix} \text{Re}\{\mathbf{x}_o\} \\ \text{Im}\{\mathbf{x}_o\} \end{bmatrix} \triangleq \sqrt{p_i} \frac{\mathbf{v}_{\max}\{\underline{\mathbf{Z}}_{ab}\}}{\|\mathbf{v}_{\max}\{\underline{\mathbf{Z}}_{ab}\}\|} \in \mathbb{R}^{2N \times 1}. \quad (20)$$

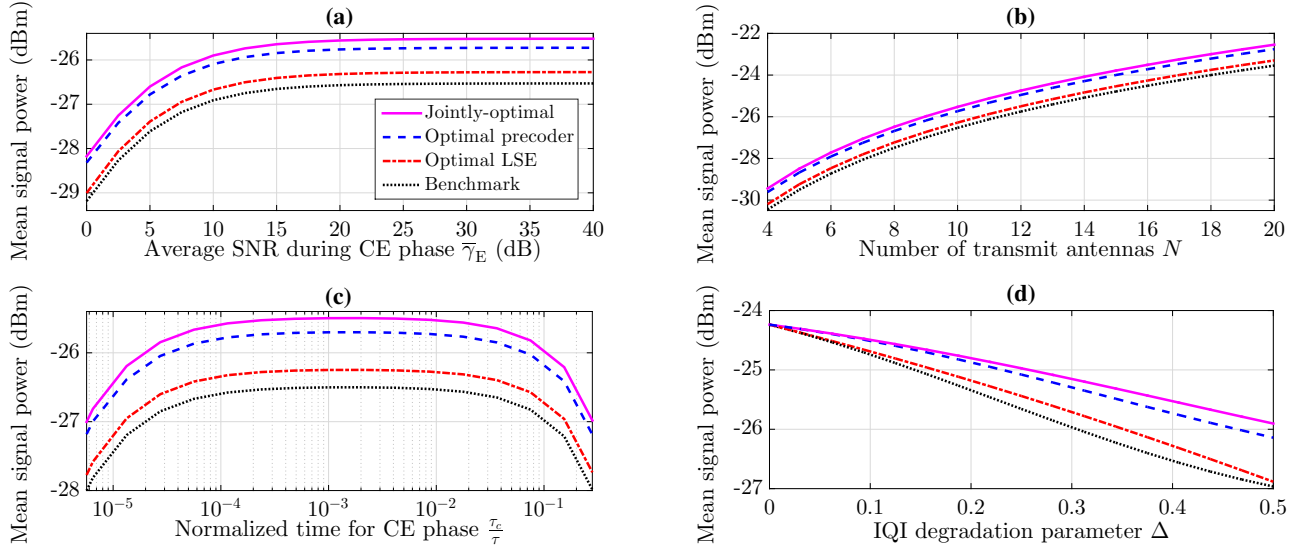


Fig. 2. Comparing relative performance of proposed optimal LSE, precoder, and jointly-optimal designs against benchmark for different $\bar{\gamma}_E$, N , τ_c , Δ values.

D. Extending Precoder Design to Multiuser Settings

For maximizing the sum received power among K single-antenna users, the precoder optimization problem is given by

$$\mathcal{O}_3: \underset{\mathbf{x}}{\operatorname{argmax}} \|\mathbf{A}\mathbf{x} + \mathbf{B}\mathbf{x}^*\|^2, \quad \text{subject to (C1),}$$

where the $K \times N$ matrices \mathbf{A} and \mathbf{B} are respectively obtained from \mathbf{a} and \mathbf{b} in (14a) and (14b), but with s_U replaced by unit-energy vector s_U , \mathbf{h} replaced with $N \times K$ matrix \mathbf{H} whose i th column corresponds to channel gain for \mathcal{S} to i th user link, and the $K \times K$ diagonal matrices \mathbf{R}_{U1} and \mathbf{R}_{U2} , respectively replacing R_{U1} and R_{U2} . Here, i th diagonal entries of \mathbf{R}_{U1} and \mathbf{R}_{U2} incorporate the RX amplitude and phase mismatch at i th user. So, following Section IV-C, the optimal precoder for \mathcal{O}_3 is given by (20), but with \mathbf{A} and \mathbf{B} respectively replacing \mathbf{a} and \mathbf{b} in \mathbf{Z}_{ab} definition. The accuracy of this TX design in multiuser setting can be verified from the fact that for no IQI, \mathbf{Z}_{ab} reduces to $\mathbf{H}\mathbf{H}^H$ with result matching [24, Theorem 1].

V. PERFORMANCE EVALUATION AND CONCLUSION

Here we numerically validate the proposed CE analysis and precoder optimization while setting simulation parameters as $N = 10$, $\tau = 10\text{ms}$, $\tau_c = 0.01\tau$, $p_i = 30\text{dBm}$, $p_c = -30\text{dBm}$, $\sigma_1^2 = \sigma_2^2 = 10^{-17}$ Joule, and $\beta = \frac{\varpi}{d^\alpha}$, where $\varpi = \left(\frac{3 \times 10^8}{4\pi f}\right)^2$ is average channel attenuation at unit reference distance with $f = 915\text{MHz}$ as TX frequency, $d = 100\text{m}$ as \mathcal{S} -to- \mathcal{U} distance, and $\alpha = 2.5$ as path loss exponent. For the average simulation results, we have used 10^5 independent channel realizations.

A. Validation of Proposed LSE under Practical IQI Modelling

We start with verifying the quality of proposed LSE $\hat{\mathbf{h}}$ (cf. (11)) in Fig. 1 against the benchmark $\hat{\mathbf{h}}_A$ as defined in (6). For IQI incorporation, we adopt the following practical model [25]

$$g \triangleq 1 - \Delta_g(1 + \Psi_g), \quad \phi \triangleq \Delta_\phi(1 + \Psi_\phi), \quad (21)$$

where g and ϕ respectively can incorporate any amplitude and phase mismatch, with the constants Δ_g and Δ_ϕ representing the errors due to fixed sources. Whereas, Ψ_g and

Ψ_ϕ , respectively denoting errors due to random sources, are assumed to follow the uniform distribution [13], [14] over the interval $[-\frac{1}{2}\Phi_g, \frac{1}{2}\Phi_g]$ and $[-\frac{1}{2}\Phi_\phi, \frac{1}{2}\Phi_\phi]$, respectively. Since the practical ranges for the constants (Δ_g , Δ_ϕ , Φ_g , Φ_ϕ) corresponding to the means and variances of amplitude and phase errors (in radians) are similar [26], [27], we set $\Delta_g = \Delta_\phi = \Phi_g = \Phi_\phi = \Delta = 0.4$, for each of the 8 IQI parameters.

Results plotted in Fig. 1 show the trend in mean square error (MSE) [1] between the actual channel \mathbf{h} and its LSE (proposed $\hat{\mathbf{h}}$ and benchmark $\hat{\mathbf{h}}_A$) against increasing average received signal-to-noise-ratio (SNR) $\bar{\gamma}_E = \frac{\beta p_c \tau_c}{\sigma_i^2}$ at \mathcal{S} during CE phase. The quality of both proposed and existing LSE improve with increasing $\bar{\gamma}_E$ because the underlying CE errors reduce for both considered values of IQI degradation parameter Δ . However, for the benchmark LSE, the error floor region starts at $\bar{\gamma}_E = 20\text{dB}$ and $\bar{\gamma}_E = 30\text{dB}$ for $\Delta = 0.4$ and $\Delta = 0.1$, respectively. Whereas, MSE for the proposed globally-optimal LSE for the IQI-impaired channel keeps on decreasing at the same rate *without* having any error floor. This corroborates the *significantly-higher* practical utility of our proposed LSE $\hat{\mathbf{h}}$ for the IQI-influenced MISO communications, in terms of our CE design providing about -3dB and -11dB improvement in MSE over benchmark for $\Delta = 0.1$ and $\Delta = 0.4$, respectively.

B. Comparison of Proposed Designs Against Benchmark

Here we compare the mean signal power performance of the three proposed schemes: (i) *jointly-optimal* LSE $\hat{\mathbf{h}}$ and precoder \mathbf{x}_o , (ii) *optimal precoder* \mathbf{x}_o with conventional LSE $\hat{\mathbf{h}}_A$, (iii) *optimal LSE* $\hat{\mathbf{h}}$ with MRT-based precoder \mathbf{x}_A , against the *benchmark* having LSE $\hat{\mathbf{h}}_A$ and precoder \mathbf{x}_A . Starting with comparison for different $\bar{\gamma}_E$ in Fig. 2(a), we notice that jointly-optimal performs the *best*, followed by optimal precoder and proposed LSE. The gaps between the optimal and benchmark designs increase with $\bar{\gamma}_E$ due to lower errors at higher SNRs.

Next in Fig. 2(b), we plot the comparison for different array sizes N at \mathcal{S} . Here, with N increased from 4 to 20, mean signal power at \mathcal{U} gets enhanced by 7dB for each of the four schemes. However, their relative gap remains *invariant* of N .

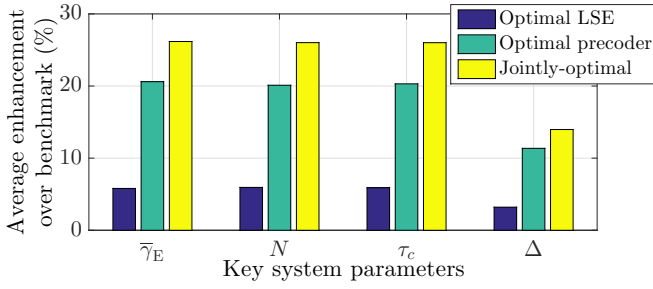


Fig. 3. Average performance gains of our proposed designs over benchmark.

Now, shifting focus to CE time τ_c , we shed insights on how to optimally set it. From Fig. 2(c), we notice that the relative trend among four schemes is similar, but more importantly, the optimal τ_c for each scheme is *practically the same* ($\approx 10^{-3}\tau$).

Next we investigate the impact of increased mismatch Δ in the amplitude and phase terms modelling the IQI. In particular, by plotting the variation of Δ from 0 to 0.5 [13], [14], [25] in Fig. 2(d), we observe that degradation in the mean signal power performance gets enhanced with increased IQI (i.e., Δ) for each scheme. However, this performance degradation for jointly-optimal, optimal precoder, optimal LSE, and benchmark schemes when parameter Δ increases from 0 (no IQI) to 0.5 is -1.6dB , -1.9dB , -2.7dB , and -2.8dB , respectively.

Lastly, in Fig. 3, we have plotted the average performance gains as achieved by the proposed LSE $\hat{\mathbf{h}}$, precoder \mathbf{x}_o , and the jointly-optimal design over benchmark for different values of critical parameters $\bar{\gamma}_E$, N , τ_c , and Δ . We observe that jointly-optimal design provides an *overall improvement of 24%*. Here, optimal precoder, providing about 18% enhancement alone in mean signal power at \mathcal{U} , proved to be a *better semi-adaptive scheme* than optimizing LSE, which yields 6% improvement.

C. Concluding Remarks

This letter exploiting the additional channel gain information in the signal received during IQI-impaired MISO communication, came up with a *novel LSE* that is shown to reduce the overall MSE in CE by -8dB , while totally *removing the error floor*. To maximize the practical EB gains in both single and multiple user set-ups, we derive new *globally-optimal precoder* in the form of *principal eigenvector* of the matrix composed of IQI parameters and LSE. Numerical results have shown that the proposed jointly-optimal LSE and precoder design can provide an overall improvement of 24% over the benchmark. This corroborates the fact that our proposed design is the *way-forward* to maximize practical utility of low-cost hardware in multiantenna transmission supported sustainable IoT systems.

REFERENCES

- [1] T. L. Marzetta, E. G. Larsson, H. Yang, and H. Q. Ngo, *Fundamentals of massive MIMO*. Cambridge, U.K: Cambridge University Press, 2016.
- [2] L. Liu, E. G. Larsson, W. Yu, P. Popovski, C. Stefanovic, and E. de Carvalho, "Sparse signal processing for grant-free massive connectivity: A future paradigm for random access protocols in the internet of things," *IEEE Signal Process. Mag.*, vol. 35, no. 5, pp. 88–99, Sept. 2018.
- [3] T. Schenk, *RF Imperfections in High-Rate Wireless Systems: Impact and Digital Compensation*. Dordrecht, The Netherlands: Springer, 2008.

- [4] X. Yang, M. Matthaiou, J. Yang, C. Wen, F. Gao, and S. Jin, "Hardware-constrained millimeter-wave systems for 5G: challenges, opportunities, and solutions," *IEEE Commun. Mag.*, vol. 57, no. 1, pp. 44–50, Jan. 2019.
- [5] A. Bereyhi, M. A. Sedaghat, S. Asaad, and R. Mueller, "Nonlinear precoders for massive MIMO systems with general constraints," in *Proc. Int. ITG Workshop on Smart Antennas (WSA)*, Berlin, Germany, Mar. 2017, pp. 1–8.
- [6] A. Bereyhi, M. A. Sedaghat, R. R. Müller, and G. Fischer, "GLSE precoders for massive MIMO systems: Analysis and applications," *CoRR*, vol. abs/1808.01880, Sept. 2018. [Online]. Available: <http://arxiv.org/abs/1808.01880>
- [7] D. Spano, M. Alodeh, S. Chatzinotas, and B. Ottersten, "Symbol-level precoding for the nonlinear multiuser MISO downlink channel," *IEEE Trans. Signal Process.*, vol. 66, no. 5, pp. 1331–1345, Mar. 2018.
- [8] A. A. DAmico, M. Morelli, and M. Moretti, "Periodic preamble-based frequency recovery in OFDM receivers plagued by IQ imbalance," *IEEE Trans. Wireless Commun.*, vol. 16, no. 12, pp. 8305–8315, Dec. 2017.
- [9] S. Wang and L. Zhang, "Signal processing in massive MIMO with IQ imbalances and low-resolution ADCs," *IEEE Trans. Wireless Commun.*, vol. 15, no. 12, pp. 8298–8312, Dec. 2016.
- [10] N. Kolomvakis, M. Coldrey, T. Eriksson, and M. Viberg, "Massive MIMO systems with IQ imbalance: Channel estimation and sum rate limits," *IEEE Trans. Commun.*, vol. 65, no. 6, pp. 2382–2396, June 2017.
- [11] S. Zarei, W. H. Gerstacker, J. Aulin, and R. Schober, "IQ imbalance aware widely-linear receiver for uplink multi-cell massive MIMO systems: Design and sum rate analysis," *IEEE Trans. Wireless Commun.*, vol. 15, no. 5, pp. 3393–3408, May 2016.
- [12] Y. Xiong, N. Wei, Z. Zhang, B. Li, and Y. Chen, "Channel estimation and IQ imbalance compensation for uplink massive MIMO systems with low-resolution ADCs," *IEEE Access*, vol. 5, pp. 6372–6388, Apr. 2017.
- [13] A. E. Canbilen, S. S. Ikki, E. Basar, S. S. Gultekin, and I. Develi, "Impact of IQ imbalance on amplify-and-forward relaying: Optimal detector design and error performance," *IEEE Trans. Commun.*, vol. 67, no. 5, pp. 3154–3166, May 2019.
- [14] Y. Xiong, N. Wei, and Z. Zhang, "An LMMSE-based receiver for uplink massive MIMO systems with randomized IQ imbalance," *IEEE Commun. Lett.*, vol. 22, no. 8, pp. 1624–1627, Aug. 2018.
- [15] S. Narayanan, B. Narasimhan, and N. Al-Dhahir, "Training sequence design for joint channel and IQ imbalance parameter estimation in mobile SC-FDE transceivers," in *Proc. IEEE ICASSP*, Dallas, TX, USA, Mar. 2010, pp. 3186–3189.
- [16] D. Mishra and H. Johansson, "Efficacy of multiuser massive MISO wireless energy transfer under IQ imbalance and channel estimation errors over rician fading," in *Proc. IEEE ICASSP*, Calgary, Canada, Apr. 2018, pp. 3844–3848.
- [17] S. A. Mohajerin and S. M. S. Sadough, "On the interaction between joint Tx/Rx IQI and channel estimation errors in DVB-T systems," *IEEE Syst. J.*, vol. 12, no. 4, pp. 3271–3278, Dec. 2018.
- [18] M. K. Simon and M.-S. Alouini, *Digital communication over fading channels*, 2nd ed. New Jersey: John Wiley & Sons, 2005, vol. 95.
- [19] Y. Zeng and R. Zhang, "Optimized training design for wireless energy transfer," *IEEE Trans. Commun.*, vol. 63, no. 2, pp. 536–550, Feb. 2015.
- [20] S. M. Kay, *Fundamentals of Statistical Signal processing: Estimation Theory*. Upper Saddle River, NJ: Prentice Hall, 1993, vol. 1.
- [21] A. Hjørungnes, *Complex-Valued Matrix Derivatives: With Applications in Signal Processing and Communications*. New York, NY, USA: Cambridge Univ. Press, 2011.
- [22] S. Yadav, P. K. Upadhyay, and S. Prakriya, "Performance evaluation and optimization for two-way relaying with multi-antenna sources," *IEEE Trans. Veh. Technol.*, vol. 63, no. 6, pp. 2982–2989, July 2014.
- [23] M. S. Bazaraa, H. D. Sherali, and C. M. Shetty, *Nonlinear Programming: Theory and Applications*. New York: John Wiley and Sons, 2006.
- [24] H. Son and B. Clerckx, "Joint beamforming design for multi-user wireless information and power transfer," *IEEE Trans. Wireless Commun.*, vol. 13, no. 11, pp. 6397–6409, Nov 2014.
- [25] D. Mishra and H. Johansson, "Optimal channel estimation for hybrid energy beamforming under phase shifter impairments," *IEEE Trans. Commun.*, vol. 67, no. 6, pp. 4309–4325, June 2019.
- [26] S. Zarei, W. H. Gerstacker, J. Aulin, and R. Schober, "IQ imbalance aware widely-linear receiver for uplink multi-cell massive MIMO systems: Design and sum rate analysis," *IEEE Trans. Wireless Commun.*, vol. 15, no. 5, pp. 3393–3408, May 2016.
- [27] D. Mishra and H. Johansson, "Efficacy of hybrid energy beamforming with phase shifter impairments and channel estimation errors," *IEEE Signal Process. Lett.*, vol. 26, no. 1, pp. 99–103, Jan. 2019.